5444–5456 *Nucleic Acids Research, 2013, Vol. 41, No. 10* *Published online 10 April 2013*
doi:10.1093/nar/gkt238

The role of DNA bending in type IIA topoisomerase function

Imsang Lee, Ken C. Dong and James M. Berger*

Department of Molecular and Cell Biology, MC 3220 University of California, Berkeley, CA 94720-3220, USA

Received January 6, 2013; Revised March 11, 2013; Accepted March 16, 2013

ABSTRACT

Type IIA topoisomerases control DNA supercoiling and separate newly replicated chromosomes using a complex DNA strand cleavage and passage mechanism. Structural and biochemical studies have shown that these enzymes sharply bend DNA by as much as 150°; an invariant isoleucine, which has been seen structurally to intercalate between two base pairs outside of the DNA cleavage site, has been suggested to promote deformation. To test this assumption, we examined the role of isoleucine on DNA binding, bending and catalytic activity for a bacterial type IIA topoisomerase, *Escherichia coli* topoisomerase IV (topo IV), using a combination of site-directed mutagenesis and biochemical assays. Our data show that alteration of the isoleucine (Ile_{172}) did not affect the basal ATPase activity of topo IV or its affinity for DNA. However, the amino acid was important for DNA bending, DNA cleavage and supercoil relaxation. Moreover, an ability to bend DNA correlated with efficacy with which nucleic acid substrates stimulate ATP hydrolysis. These data show that DNA binding and bending by topo IV can be uncoupled, and indicate that the stabilization of a highly curved DNA geometry is critical to the type IIA topoisomerase catalytic cycle.

INTRODUCTION

DNA topoisomerases are enzymes that resolve topological problems in host chromosomes arising from natural transactions such as replication and transcription. Although extant throughout the three domains of cellular life and certain viruses, this broad superfamily of proteins can be divided into several subclasses on the basis of structure and mechanism (1,2). Type IIA topoisomerases, which include eukaryotic topoisomerase II (topo II) and the prokaryotic enzymes, DNA gyrase and topoisomerase IV (topo IV), play a critical role in maintaining supercoiling homeostasis and disentangling daughter chromosomes following replication (3). Topo II is formed by the dimerization of a single polypeptide chain, whereas the homologous gyrase and topo IV proteins are A_2B_2 heterotetramers formed by two subunit pairs (GyrA/GyrB and ParC/ParE, respectively). All type IIA topoisomerases contain a Gyrase, Hsp90, Histidine Kinase, MutL (GHKL) ATPase domain (4–6), a metal-binding topoisomerase-primase (TOPRIM) fold (7) and an internal winged-helix domain (WHD) (8,9); the latter two elements comprise a central DNA binding and cleavage core (Figure 1A) (8,10,11). When assembled in the context of the topoisomerase holoenzyme, these disparate domains work together to create three separable subunit interfaces (termed 'gates') that facilitate the controlled passage of one DNA duplex (the Transfer or T-segment) through a transient double-stranded break in a second DNA duplex (the Gate or G-segment) (12–15). Actuation of specific interfacial gates is controlled by an allosteric relay mechanism that links ATP binding and hydrolysis to DNA cleavage and strand passage, and *vice versa* (13,16,17).

The first crystallographic view of the DNA binding and cleavage core of topo II bound to a G-segment DNA showed that the enzyme severely bent the DNA duplex (Figure 1B) (18). Deformation was proposed to be mediated by a β-hairpin element, which was observed to wedge into the DNA minor groove and insert an invariant isoleucine (Ile_{833} in *Saccharomyces cerevisiae* topo II) between two adjacent base pairs (Figure 1C). The combined action of the two isoleucines in the topo II homodimer appeared to promote bending of the DNA by ~150°. Despite a complete lack of primary sequence or tertiary structure conservation, this mechanism of deformation proved unexpectedly congruent with the approach used by the bacterial integration host factor (IHF) and the HU protein, which use a β-hairpin motif bearing a proline to bend DNA (19,20).

*To whom correspondence should be addressed. Tel: +1 510 643 9483; Fax: +1 510 643 9290; Email: jmberger@berkeley.edu
Present address:
Ken C. Dong, Department of Structural Biology, Genentech Inc. South San Francisco, CA 94080, USA.

The authors wish it to be known that, in their opinion, the first two authors should be regarded as joint First Authors.

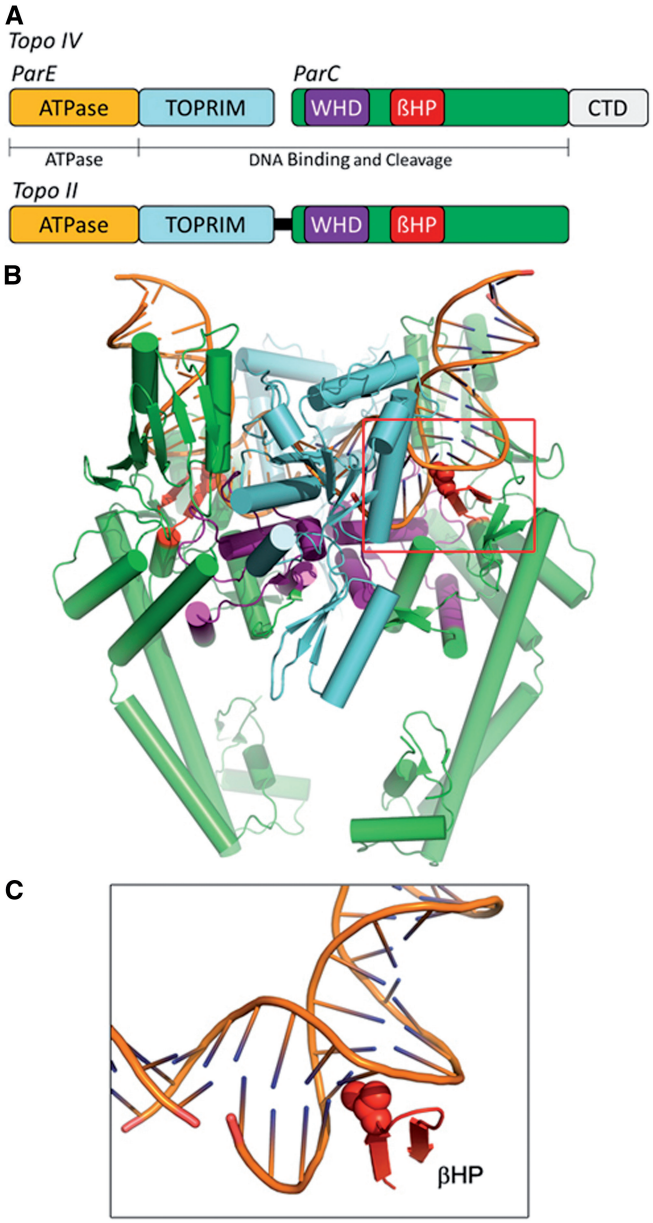

Figure 1. Type IIA topoisomerase organization. (**A**) Domain arrangement of *E. coli* topo IV and *S. cerevisiae* topo II. Functional regions are colored and labeled. (**B**) DNA bending by type IIA topoisomerase as revealed by the crystal structure of a noncovalent *S. cerevisiae* topo II•DNA complex (PDB entry 2RGR). Domains are colored as in (A). The bending site is highlighted by a red rectangle. (**C**) Close-up view of the bending site. The intercalating isoleucine is shown as spheres.

Subsequent crystal structures of eukaryotic and prokaryotic type IIA topoisomerases bound to DNA in various cleaved and uncleaved states have recapitulated the configuration between the isoleucine and duplex DNA seen initially in yeast topo II (21–24). Multiple orthogonal studies—including J-factor analysis (25), Förster Resonance Energy Transfer (FRET) (26), electron microscopy (25,27), and atomic force microscopy (AFM) (26)—likewise have found evidence for DNA bending. However, despite this agreement, no work has yet probed the link between the conserved isoleucine and DNA bending, or shown whether bending is necessary for the function of type IIA topoisomerases in general.

To address these issues, we carried out a set of biochemical studies on variants of *Escherichia coli* topo IV containing either substitutions for the conserved isoleucine (Ile_{172}), or deletion of this residue's associated β-hairpin. Analysis of these mutants showed that even highly conservative alterations are deficient in relaxing or cleaving supercoiled DNA. Fluorescence studies with labeled linear DNA oligos show that both an intact β-hairpin and Ile_{172} are required for wild-type (WT) levels of DNA bending, but that the isoleucine is dispensable for DNA binding. Surprisingly, isoleucine substitutions that support wild-type levels of DNA binding also show defects in DNA-stimulated ATPase activity, with a progressive loss of stimulation observed as bending becomes increasingly impaired by more severe mutations. Together, these results establish a key role for Ile_{172} in the formation and maintenance of a bent DNA state, and demonstrate that the ability to bend DNA is necessary to support normal type IIA topoisomerase function.

MATERIALS AND METHODS

Mutagenesis

Site-directed mutagenesis was performed using the Quikchange mutagenesis kit (Stratagene, Santa Clara, CA, USA) on a modified pET28b plasmid containing a ParC overexpression construct (28). Primers for mutagenesis were obtained from Integrated DNA Technology (IDT, Coralville, IA, USA). Sequences of primers used can be found in Supplementary Table S1. Insertion of desired mutation was verified by DNA sequence determination (UC Berkeley Sequencing Facility).

Expression and purification

Escherichia coli ParC and ParE were expressed as an N-terminally His_6-tagged protein in *E. coli* BL21-Codon Plus(DE3)-RIL cells (28). Both proteins were purified using Ni^{2+} affinity chromatography, followed by tobacco etch virus protease cleavage of the His-tag, a second Ni^{2+} column, and size-exclusion chromatography (Sephacryl S-300, GE Healthcare, Piscataway, NJ, USA), as described previously (28). All of the ParC mutant proteins were soluble and well behaved during purification. To assemble the topo IV tetramer, equimolar amounts of ParC and ParE were mixed and incubated for 30 min at 4°C, as described previously (28). This assembled complex was subsequently used to perform the experiments described below.

DNA cleavage

Reactions were carried out as described previously (29). Briefly, 200 ng of supercoiled pUC19 plasmid DNA were incubated for 25 min at 37°C with topo IV in a total of 20 µl of buffer (10 mM Tris–HCl (pH 7.6), 50 mM KCl, 50 mM NaCl) that contained 5 mM $CaCl_2$. Negatively supercoiled pUC19 was purified from *E. coli* XL1 Blue cells using a MaxiPrep kit (Qiagen, Valencia, CA, USA).

To quench the reaction, 2 µl of 0.8 mg/ml of proteinase K, 1 µl 250 mM EDTA and 2 µl 5% sodium dodecyl sulphate (SDS) were added, and the mixture was allowed to incubate at 45°C for 30 min to digest topo IV. Reaction products were resolved by electrophoresis on 1% Tris-acetate-EDTA (TAE) agarose gels (Invitrogen, Carlsbad, CA, USA) at 2 V/cm, and then stained for 15 min in an aqueous solution of ethidium bromide (0.5 µg/ml). DNA bands were visualized by transillumination with ultraviolet light (300 nm) and photographed using EDAS 290 gel imaging system (Kodak, Rochester, NY, USA).

Supercoiled DNA relaxation

pUC19 plasmid DNA was used for supercoiled substrates. Positively supercoiled DNA was made using *A. fulgidus* reverse gyrase (30). DNA supercoil relaxation assays were performed using a modification of the method used by (31). Briefly, 0–200 nM topo IV was added to a 50 µl reaction containing 300 ng negatively or positively supercoiled pUC19 in 50 mM Tris–HCl (pH 7.6), 6 mM $MgCl_2$, 10 mM DTT, 1 mM ATP and 20 mM KCl, and incubated at 37°C for 25 min. Reactions were stopped with SDS (1% final) and EDTA (10 mM final) and analyzed by electrophoresis on 1% TAE agarose gels (Invitrogen) at 2 V/cm for 14–16 h. Gels were stained and visualized as described for the DNA cleavage assays. To determine relative activities of topo IV on different substrates, we quantified the amounts of supercoiled DNA in each lane using ImageJ (32) and plotted the relative amount of supercoiled DNA remaining versus the molar ratio of topo IV:DNA.

ATPase activity

ATP hydrolysis rates were measured using a modified coupled ATPase assay (33,34). Reactions of 100 µl were set up with 50 nM topo IV with 5 U pyruvate kinase, 8 U lactate dehydrogenase (PK/LDH, Sigma Aldrich, St Louis, MO, USA) and 0.5 mM phosphoenol pyruvate (Sigma Aldrich), along with 0.1 mM nicotinamide adenine dinucleotide, reduced disodium salt (NADH, Sigma Aldrich), 50 mM HEPES-KOH, pH 7.5, 150 mM potassium acetate, 8 mM magnesium acetate, 5 mM β-mercaptoethanol and 100 µg/ml bovine serum albumin (BSA). Reactions were followed by absorbance in 96-well plates using a Victor 3V plate reader (Perkin Elmer, Waltham, MA, USA) at 340 nm (band pass 8 nm) with and without 25 µM (base pair concentration) of pUC19. Adenosine 5′-triphosphate (ATP, Sigma Aldrich) concentration was varied from 0 to 4 mM. An experimentally defined extinction coefficient was empirically calculated for NADH for the plate reader as 2701.9 M^{-1}, and was used to calculate the turnover rate by fitting to the linear portion of the activity curve. K_m and V_{max} were calculated by fitting the data to the Michaelis–Menten kinetics in Prism 5 (Graphpad software, La Jolla, CA, USA).

DNA binding

Two strands of DNA with a strong DNA cleavage site based on sequences used for testing cleavage by topo II were obtained from IDT and annealed (35).

One strand contained a 5′-fluorescein dye:

5′-CCATTCGCTGTATGACGATGCGCGCATCGTCA TCCTCGGATAGGC-3′.

The other has the following sequence:

5′-GCCTATCCGAGGATGACGATGCGCGCATCGT CATACAGCGAATGG-3′.

DNA-binding experiments were performed using fluorescence anisotropy (FA). Topo IV was titrated (0–1000 nM) against a 20 nM solution of fluorescein-labeled DNA in 25 mM Tris–HCl (pH 7.6), 20 mM NaCl, 10 mM $MgCl_2$, 10% glycerol and 100 µg/ml BSA (Buffer A). Final reaction volumes were 20 µl.

Fluorescence measurements were performed on a Victor3V plate reader using a 480 nm excitation (band pass 30 nm) and 535 nm emission (band pass 40 nm) filter set, and the data fit to a single site-binding model incorporating the concentration of DNA in Prism 5 [Equation (1), (36)]:

$$F_b = \frac{Kd + P + L - \sqrt{(Kd + P + L)^2 - 4 \times P \times L}}{2 \times L} \quad (1)$$

where F_b = fraction bound, and P and L are the total protein and ligand concentrations, respectively.

FRET DNA-bending experiments

The same sequence was used as with the DNA-binding experiments, except that the labels were changed as follows:

(strand 1)

5′-Cy3-CCATTCGCTGTATGACGATGCGCGCATCG TCATCCTCGGATAGGC-3′.

(strand 2)

5′-Cy5-GCCTATCCGAGGATGACGATGCGCGCAT CGTCATACAGCGAATGG-3′.

For the assay, 0–1000 nM topo IV was titrated against 100 nM labeled DNA in 14 µl reactions containing buffer A. Emission spectra (545–700 nm) were measured after excitation of Cy3 by 530 nm light using Fluoromax fluorometer 4 (HORIBA Jobin Yvon, Edison, NJ, USA).

For analyzing the FRET data, the donor emission maximum obtained for each experiment was first scaled to a normalized value of 1.0. Each point on a given curve was then multiplied by the scaling factor used to normalize its maximal donor emission value. This treatment has the effect of placing all measured donor emission maxima (and their associated FRET spectra) on the same absolute scale with respect to each other. To calculate bend angles, we then followed the procedure of Neuman and co-workers (26). The overall bend was modeled as two symmetric bends (each with angle θ/2) on either side of a short DNA segment of length r_c, which in turn sits between two dyes separated by a total distance r_{tot}, along the DNA (Figure 5C). The FRET efficiency (E) between donor and acceptor was calculated as the ratio of the donor fluorescence intensity of the singly labeled

substrate (F_D) compared with the donor fluorescence intensity of doubly labeled substrate (F_{DA}) using Equation (2):

$$E = 1 - \frac{F_{DA}}{F_D} = 1 - \frac{F_{complex}}{F_{DNA}} \quad (2)$$

Because F_D is unchanged in the presence of topo IV, and because we determined that F_D and F_{DA} were identical in the absence of topo IV (not shown), F_D can be obtained from the donor intensity of the doubly labeled substrate without topo IV (F_{DNA}); under these conditions, E from the complex with topo IV can be obtained by the ratio of the donor intensity of doubly labeled substrates, with ($F_{complex}$) and without topo IV (F_{DNA}). The distance between the fluorophores (r) was determined from these FRET efficiency measurements using Equation (3):

$$r = R_0\left[\frac{1-E}{E}\right]^{1/6} \quad (3)$$

with R_0 value of 5.4 nm for the Cy3–Cy5 fluorophore pair. The overall bend angle (θ) was then calculated using Equation (4):

$$r = \sqrt{\left|r_c + (r_{tot} - r_c)\cos(\theta/2)\right|^2 + r_{rise}^2} \quad (4)$$

which describes the relationship between r and the geometry of the bent DNA (26). As per Hardin *et al.*, we assumed the DNA geometry was similar to that observed in crystal structures (18,21,37,38), with $r_c = 4.8$ nm, $r_{tot} = 15$ nm and $r_{rise} = 1.5$ nm.

The FRET efficiencies calculated from above were also used to directly compare the relative ability of each isoleucine mutant with bend DNA with respect to wild-type topo IV.

RESULTS

Ile_{172} variants are defective for relaxing DNA supercoils

Escherichia coli topo IV is a potent decatenase and a robust relaxase of positive supercoils (39,40). Topo IV also will relax negatively supercoiled DNA, but at a slower rate (41). To begin to assess the role of the conserved isoleucine (Ile_{172}) on topo IV function, we created a series of substitutions ranging from conservative (Ile→Val, Ile→Leu) to relatively severe (Ile→Ala, Ile→Gly, Ile→Trp). Because IHF uses a proline to introduce bends into DNA, we also created an Ile→Pro mutation. Each of these mutants was purified as per the wild-type enzyme and then tested for various activities (See 'Materials and Methods' section).

We first asked whether Ile_{172} variants could relax negatively supercoiled DNA. A serial dilution of topo IV (0–200 nM) was added to 300 ng of negatively supercoiled pUC19 and allowed to act on the substrate for 25 min at 37°C, after which the resulting plasmid topoisomers were resolved by native gel electrophoresis. This experiment showed that the Ile_{172}Val, Ile_{172}Leu and Ile_{172}Pro substitutions were less effective at supercoil removal, requiring 4-fold, 8-fold and ≥20-fold more enzyme, respectively, to relax DNA to a similar extent as the native protein (Figure 2). The more severe isoleucine mutants in our panel (Ile_{172}Ala, Ile_{172}Gly and Ile_{172}Trp) showed no activity under our assay conditions, even when present at a 50-fold molar excess over the DNA substrate (Figure 2, Supplementary Figure S1). As an additional test, we found that a mutant containing a deletion of the β-hairpin that bears Ile_{172} (Δhp, spanning residues 171–178) likewise completely abrogated relaxation activity (Supplementary Figure S1).

To investigate the role of Ile_{172} further, we next asked how mutations at this position affected topo IV activity on positively supercoiled DNA, one of enzyme's preferred substrates. As observed previously, wild-type topo IV proved much more active on this DNA form than on a negatively supercoiled plasmid (41) (Figure 3A). However, the Ile_{172} variants again displayed reduced levels of activity, with the Ile_{172}Val and Ile_{172}Leu mutants requiring even greater amounts of enzyme (~10-fold and ≥20-fold, respectively) to relax substrate to a similar degree as wild-type topo IV when compared with negative-supercoil relaxation assays (Figure 3, Supplementary Figure S2). Thus, even on a more ideal DNA substrate, substitutions to Ile_{172} still significantly and adversely impact the relaxation activity of topo IV.

Amino acid identity at position 172 plays a role in supporting DNA cleavage

Because supercoil relaxation requires a suite of activities to work together in concert—DNA binding, DNA cleavage, ATP turnover—we set out to define which steps in the topo IV catalytic cycle specifically required an isoleucine at the site of the DNA bend. We first examined DNA cleavage (see 'Materials and Methods' section). During strand passage, type IIA topoisomerases form a transient double-stranded DNA break through the formation of a phosphotyrosine reaction intermediate (42–44). Reversal of this cleaved state can be blocked by the addition of calcium, trapping a covalent protein–DNA complex (29). Denaturation and degradation of the topo IV can be accomplished by the addition of SDS and proteinase K, generating linear DNA that can be distinguished from a starting supercoiled substrate using native agarose gels. Treatment of DNA with wild-type topo IV in this manner led to the expected production of linear DNA in an enzyme concentration-dependent manner (Figure 4A). Interestingly, the conservative isoleucine substitutions Ile_{172}Val and Ile_{172}Leu resulted in only a ~2-fold and 4-fold increase in the amount of enzyme required to cleave ~50% of the starting DNA substrate compared with the wild-type protein (Figure 4B and C). By contrast, the other isoleucine variants (Ile_{172}Pro, Ile_{172}Ala, Ile_{172}Gly and Ile_{172}Trp) failed to generate any cleaved intermediate, even at the highest concentration tested (Figure 4, Supplementary Figure S3). Hence, DNA cleavage by topo IV is somewhat tolerant of modest changes to Ile_{172}; however, the amino acid also plays an integral part in supporting strand scission. These data indicate that the defects seen for Ile_{172}

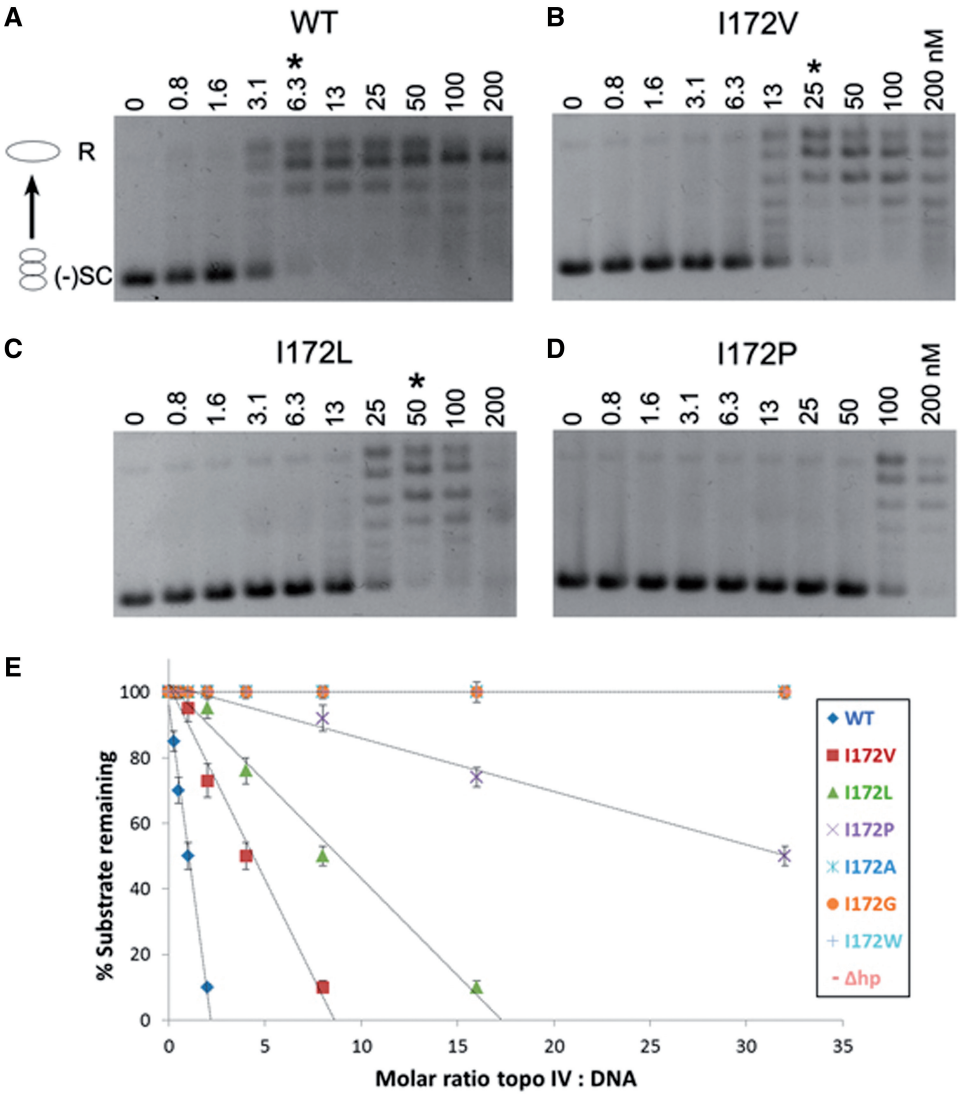

Figure 2. Ile_{172} mutants impede the relaxation of negatively supercoiled DNA. Supercoil relaxation reactions variously contained (**A**) wild-type topo IV, (**B**) Ile_{172}Val, (**C**) Ile_{172}Leu or (**D**) Ile_{172}Pro. Reconstituted wild-type or mutant topo IV was incubated at various concentrations (indicated above each lane, in nM topo IV) with negatively supercoiled plasmid DNA. The position of supercoiled DNA is indicated on the left side of the panel by 'SC', and relaxed topoisomers by 'R'. Asterisks indicate enzyme concentrations that exhibit comparable levels of activity between wild-type and mutant topo IV constructs. (**E**) Plot of the relative changes observed in supercoiled substrate as a function of the molar ratio of enzyme to DNA for each of the mutants.

mutants in DNA supercoil relaxation likely arise at least in part from impaired DNA cleavage activity, particularly for more severe substitutions.

Ile_{172} is necessary for DNA bending, but not binding

Although Ile_{172} comprises only a small fraction of the primary DNA-binding surface of topo IV (<9%), we realized that the cleavage defects seen on mutating this site might arise either from an inability to bend DNA or from a loss of binding altogether. To differentiate between these possibilities, we turned first to fluorescence anisotropy (FA) for assessing DNA affinity. For a substrate, we designed an intact 45-bp duplex DNA containing a strong type IIA topoisomerase-binding sequence and bearing a 5′-end fluorescein label (18,35). We then titrated wild-type topo IV against a constant amount of this labeled DNA (20 nM) and measured the change in the anisotropy of observed fluorescence from the dye (see 'Materials and Methods' section). Fitting the data to a general single site-binding model yielded an apparent K_d for DNA binding of 41 ± 5 nM (Figure 5A), a value in close agreement with that reported for topo IV using filter binding (28,45). As controls, we also measured the binding of DNA to ParC, ParE and the isolated CTD of ParC (consisting of residues 498–752). ParC and its isolated CTD bound DNA with $K_{d,app}$ of ~150 nM and ~200 nM, respectively, whereas ParE showed little appreciable affinity for DNA (Supplementary Figure S4). The higher affinity of full-length topo IV for DNA than either ParC or the ParC CTD alone can be explained by the observation that the

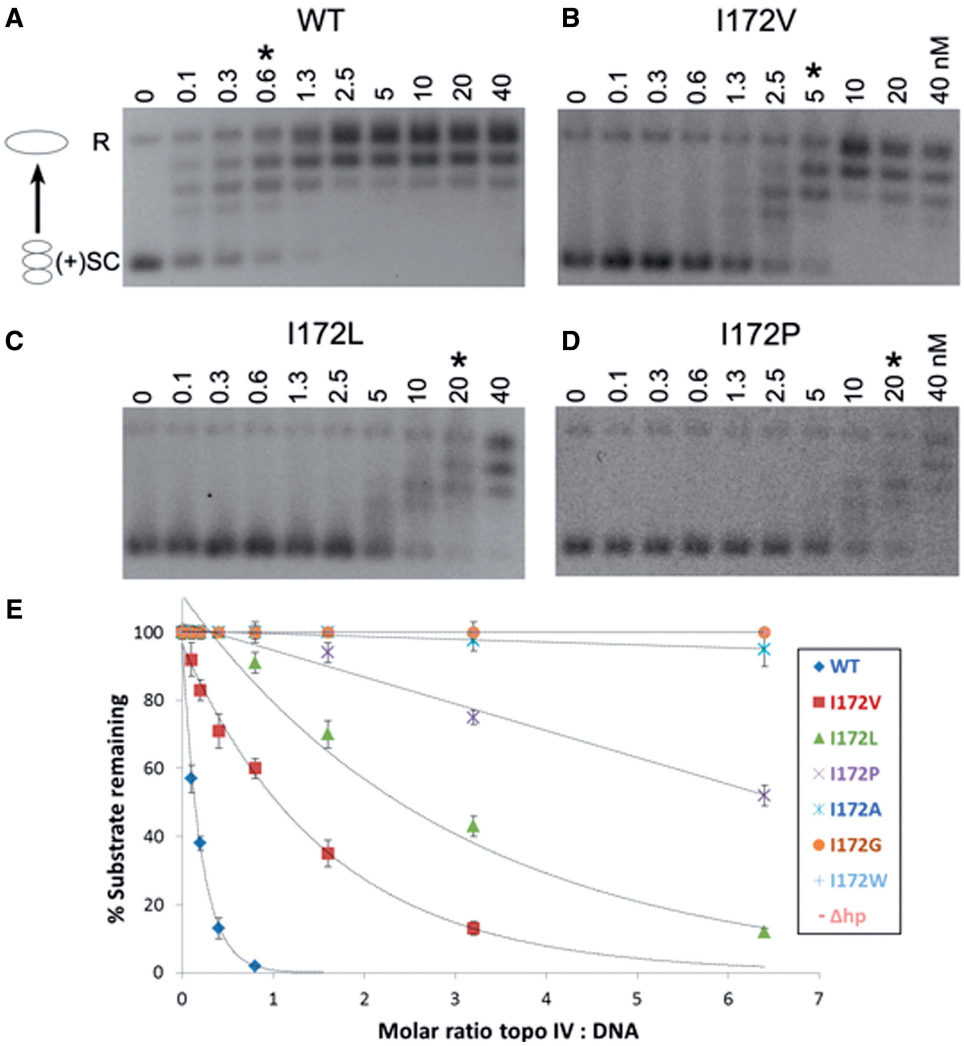

Figure 3. Ile_{172} mutants impede the relaxation of positively supercoiled DNA. Supercoil relaxation reactions variously contained (**A**) wild-type topo IV, (**B**) Ile_{172}Val, (**C**) Ile_{172}Leu or (**D**) Ile_{172}Pro. Reconstituted wild-type or mutant topo IV was incubated at various concentrations (indicated above each lane, in nM topo IV) with positively supercoiled plasmid DNA. The position of supercoiled DNA is indicated on the left side of the panel by 'SC', and relaxed topoisomers by 'R'. Asterisks indicate enzyme concentrations that exhibit comparable levels of activity between wild-type and mutant topo IV constructs. (**E**) Plot of the relative changes observed in supercoiled substrate as a function of the molar ratio of enzyme to DNA for each of the mutants.

C-terminal region of ParE, the TOPRIM fold, forms part of the nucleolytic center along with the N-terminal WHD of ParC; together, these elements form an extended positively charged groove for binding DNA whose total surface area is significantly larger than that of the isolated domains (21,23). The combined action of the TOPRIM and WHD elements dominates the DNA-binding profile of topo IV, although the CTDs, which bind DNA ~3-fold more weakly than the central core, also contribute to the total amount of DNA bound by the protein (28).

We next assessed the ability of our Ile_{172} mutants to bind DNA (Figure 5A). Using the same FA assay, we found that the $K_{d,app}$ measured for each construct was within 2–3-fold of wild-type, indicating that the substitutions had no major effect on DNA affinity (Table 1). Surprised by this tight congruency in light of their functional defects, we measured DNA-binding properties of the β-hairpin deletion mutant (Δhp) as well. Although this construct purified and behaved as per the wild-type protein by size-exclusion chromatography, it associated with DNA less tightly than native topo IV or the Ile_{172} point mutants (Figure 5A). Thus, whereas Ile_{172} does not appear to play a role in controlling the affinity of topo IV for DNA, the β-hairpin appears to contribute more substantially the binding of nucleic acid substrates.

To examine DNA bending, we next turned to FRET, using the same 45-bp duplex DNA, but now labeled on opposite 5′-ends with a Cy3/Cy5 dye pair. This length of DNA was chosen so that an unbent substrate would exhibit a dye-to-dye distance that exceeds the known Förster spacing for Cy3/Cy5 (~54 Å) (46); bending of the DNA by ~150° would be expected to shorten the distance between dyes, giving rise to FRET (Figure 5B). We first tested whether wild-type topo IV would bend this substrate

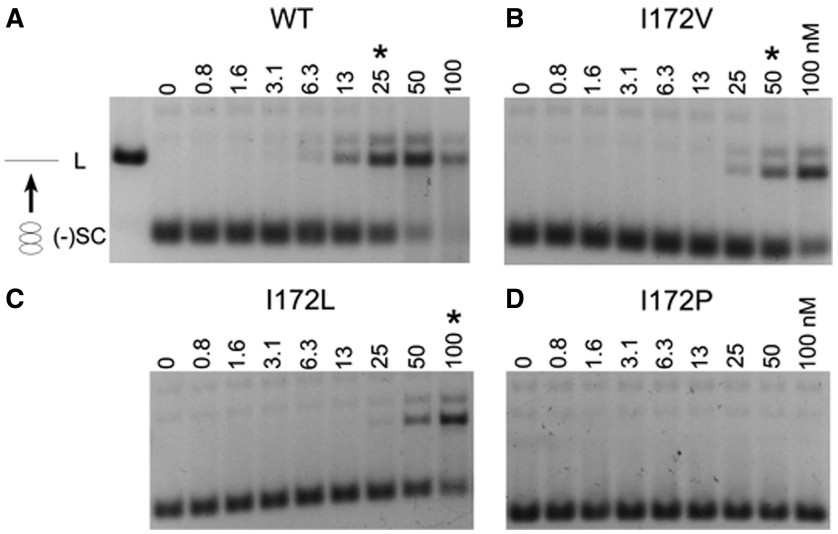

Figure 4. Ile_{172} mutants are defective for DNA cleavage. DNA cleavage reactions variously contained (**A**) wild-type topo IV, (**B**) $Ile_{172}Val$, (**C**) $Ile_{172}Leu$ and (**D**) $Ile_{172}Pro$. Reconstituted wild-type or mutant topo IV was incubated at different concentrations (indicated above each lane, in nM topo IV) with negatively supercoiled plasmid DNA. The position of the supercoiled starting substrate is indicated on the left side of panel by 'SC', and the cleaved DNA as 'L' (for "linear")'. Asterisks indicate enzyme concentrations that exhibit comparable levels of activity between wild-type and mutant topo IV constructs.

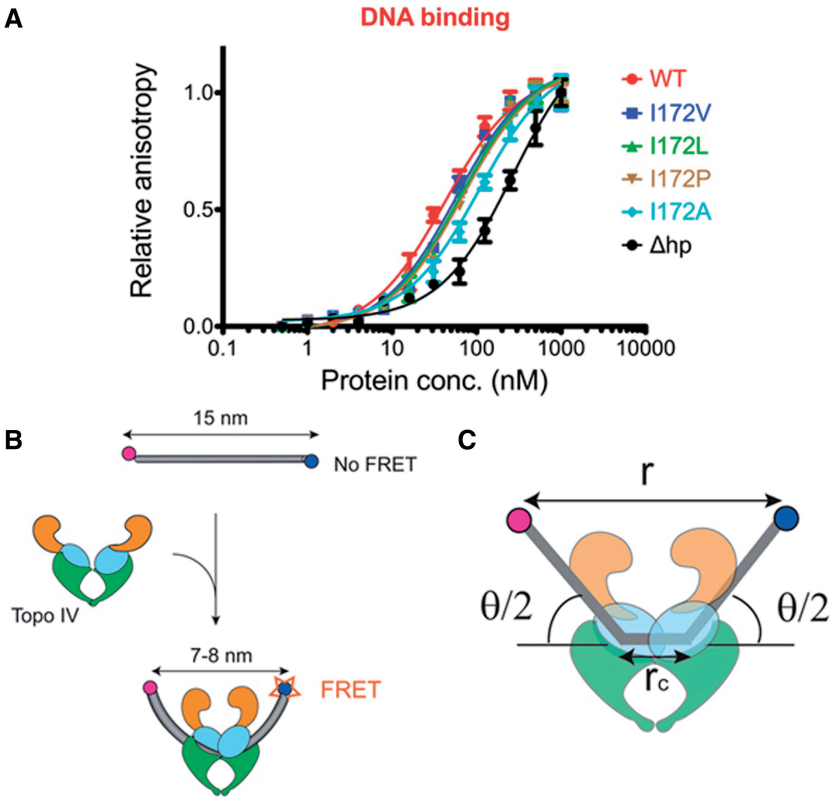

Figure 5. DNA binding and bending by topo IV. (**A**) Concentration-dependent binding of topo IV to a short duplex DNA oligo (as measured by fluorescence anisotropy). Data points represent the average of triplicate readings, and error bars represent standard deviations. (**B**) Schematic of DNA bending and the predicted distance between the dyes when the DNA is bent or unbent. (**C**) Schematic representation of DNA bending by a type IIA topoisomerase as adapted from Hardin *et al.* (26) for use in calculating bend angles. θ is the overall bend angle, r is the distance between the two fluorophores, r_c is the length of the unbent DNA segment between the two bent DNA segments and r_{tot} (not labeled) is the total distance along the DNA.

by exciting the enzyme-DNA solution at the donor wavelength (Cy3, $\lambda_{ex} = 530$ nm), followed by scanning for the emission of the acceptor dye (Cy5, $\lambda_{em,max} = 660$ nm). Individual measurements were taken at successively higher enzyme concentrations (up to and past the observed K_d for binding) to ensure that all of the DNA substrate would be fully bound, and presumably fully bent, at the highest concentrations tested. When conducted for wild-type topo IV, the fluorescence at the emission wavelength of the acceptor dye could be seen to smoothly increase as the relative amount of bent species accumulated in an enzyme concentration-dependent manner (Figure 6A). This trend indicates that the two dye moieties move closer upon stable binding of the DNA by topo IV, consistent with formation of a protein-dependent bend. Calculation of the distance between the Cy3 and Cy5 probes yielded a spacing of ~70 Å in the presence of wild-type topo IV; based on the length of DNA used and the known doubly kinked mode seen on binding DNA (Figure 5C), this value corresponds to an overall bend angle of ~150° (see 'Materials and Methods' section). Both values are in good agreement with FRET and AFM data for DNA bending by type II topoisomerases observed previously (26).

Having established that our DNA substrate recapitulates the bending seen by other groups for native topo

Table 1. DNA binding by topo IV, components of topo IV and mutants

Topo IV	Kd (nM)
$ParC_2ParE_2$	41 ± 5
ParC	152 ± 23
ParE	N.D.
ParC CTD	205 ± 37
$Ile_{172}Val$	57 ± 9
$Ile_{172}Leu$	64 ± 9
$Ile_{172}Pro$	68 ± 11
$Ile_{172}Ala$	107 ± 14
$Ile_{172}Gly$	153 ± 20
$Ile_{172}Trp$	137 ± 19
Δhp	>1000

N.D., not determined.

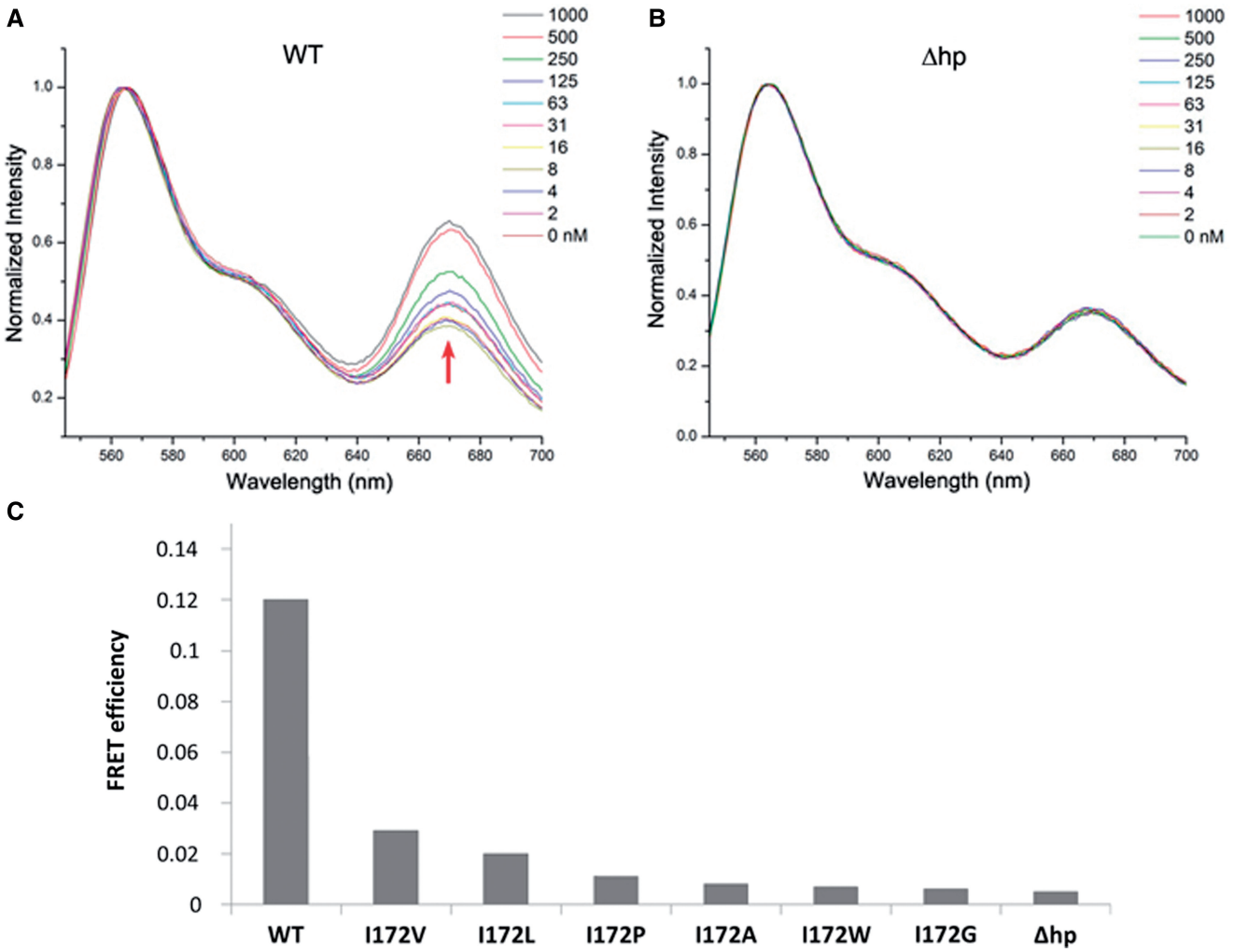

Figure 6. Ile_{172} is critical for topo IV-mediated DNA bending as reported by FRET. Fluorescence emission spectra are shown for (**A**) wild-type topo IV or (**B**) the Δhp construct. The red arrow denotes change in FRET signal that occurs on binding the DNA substrate. Spectra were obtained as described in 'Materials and Methods' section at various protein concentrations (nM, indicated in the inset). (**C**) Bar graph comparing the calculated FRET efficiencies from (A) wild-type topo IV, (B) Δhp and other variants ('Materials and Methods' section, Supplementary Figure S5).

IV (21,23,25,26), we next examined the effects of variant enzymes containing substitutions for Ile_{172} or lacking the β-hairpin entirely. As expected, based on its binding defect, the Δhp construct did not give rise to any change in FRET compared with wild-type topo IV (Figure 6B), indicating that the protein was unable to bend DNA. Notably, the most severe mutants tested (Ile_{172}Ala, Ile_{172}Gly and Ile_{172}Trp) also produced little or no detectable FRET increase, even at concentrations well above their measured K_d (Figure 6C, Supplementary Figure S5). This finding demonstrates that, although correlated, DNA binding and bending are distinct properties that can be uncoupled from one another.

The behavior of the conservative Ile_{172} mutants was more subtle, but also informative. Like wild-type topo IV, both Ile_{172}Val and Ile_{172}Leu were capable of generating an increase in FRET at the highest concentrations tested (Figure 6C, Supplementary Figure S5). However, the degree of increase was markedly smaller (75 and 83%, respectively, based on the calculated FRET efficiencies; see 'Materials and Methods' section) than that seen for the native protein. Calculation of the distances between the probes indicates that both substitutions bend DNA less extensively, on the order of ~120° for the valine mutation and ~110° for the leucine substitution (see 'Materials and Methods' section). Interestingly, titrations with Ile_{172}Pro, which corresponds to one of the most severe substitutions still capable of showing residual relaxation activity, also produced a slight FRET increase, corresponding to an even shallower bend (~90–100°, the limit of detection for a DNA substrate of this length). In general, the greater the defect seen in DNA bending by a given mutant correlates with progressively impaired supercoil relaxation and DNA cleavage functions. Thus, DNA bending is not only important for supporting strand scission and passage by topo IV, but the extent of the bend imposed by the enzyme also is critical.

DNA-stimulated ATPase activity requires DNA bending

Type IIA topoisomerases rely on ATP binding and hydrolysis to promote strand passage (47–50). DNA is not a passive participant in this reaction, as its binding is known to stimulate the rate of ATP hydrolysis by as much as ~20-fold (33,51). Similarly, the addition of nucleotide is known to significantly stimulate DNA cleavage (52). This reciprocity suggests that the ATP- and DNA-dependent activities of type IIA topoisomerases are tightly coupled. How coupling is established, however, is not fully understood.

The ability to separate DNA binding from bending using our Ile_{172} mutants afforded us with a new window for exploring the interplay between DNA and ATP turnover. In particular, we were intrigued as to whether reduction of strand passage activity seen upon altering the intercalative residue resulted solely from an inability of mutant topo IV proteins to properly bend, and hence cleave DNA, or whether bending defects might also have adversely impacted ATP hydrolysis. To investigate this question, we assessed the behavior of our mutants using a coupled ATPase assay (33,34). Control experiments with wild-type topo IV recapitulated the low-level DNA-independent activity for the enzyme, corresponding to the enzyme's basal turnover rate (Figure 7A). In turn, the addition of supercoiled plasmid DNA resulted in a marked stimulation of ATPase activity (Figure 7B). Both curves were fit well by a standard Michaelis–Menten treatment of the data, which showed that the V_{max} increased nearly 19-fold, while the K_m decreased 1.5-fold in the presence of a nucleic acid substrate (Table 2). This DNA-dependent effect accords with similar studies conducted previously not only for topo IV (53), but also for topo II and gyrase (33,51).

The mutant proteins displayed an altogether different behavior. The basal ATPase rates of all the mutants tested—Ile_{172}Val, Ile_{172}Leu, Ile_{172}Pro, Ile_{172}Ala—were all comparable with that seen for wild-type topo IV (Figure 7A), indicating that alteration of the isoleucine did not corrupt the general integrity of the hydrolytic reaction. By contrast, all of the mutants showed a decreased response in ATP turnover when DNA was present (Figure 7B, Table 2). Notably, the severity of the ATPase defects followed the same trend as seen for supercoil relaxation, DNA cleavage and DNA bending: mutants that were the least defective in bending exhibited higher turnover rates than mutants that could not bend DNA at all (Figure 7C). These findings help explain why the relatively subtle effects on DNA cleavage seen for the least severe substitutions (Ile_{172}Val and Ile_{172}Leu) have more significant effects on supercoil relaxation (compare Figure 3B and C with Figure 4B and C), as these mutants exhibit ATPase defects as well. Together, these data indicate that, as with other topo IV activities, the ability to bend DNA plays an important role in activating nucleotide hydrolysis in support of general topo IV function.

DISCUSSION

The role of Ile_{172} in DNA bending

To facilitate chromosome unlinking and changes in DNA supercoiling status, type IIA topoisomerases grip and open one double-stranded DNA while navigating a second duplex through the break (47,48). Both biochemical and structural studies have established that type IIA topoisomerases significantly bend the DNA segment that is transiently cleaved during this reaction (18,21–27,38). In instances where the substrate has been imaged in complex with the DNA binding and cleavage core of these enzymes, a pair of isoleucines has been seen to intercalate into the bound duplex, generating symmetrical kinks. The universality of this feature across type IIA topoisomerases, from bacteria to humans, has suggested that bending is critical to type IIA topoisomerase function. However, the molecular rationale for establishing a bend, and the role of this deformation in supporting topoisomerase activity, has remained unknown.

DNA bending has been proposed to be a key element in the curious ability of type IIA topoisomerases to 'simplify' topology (25,54), a process by which the enzyme narrows the steady-state distribution of DNA topoisomers or

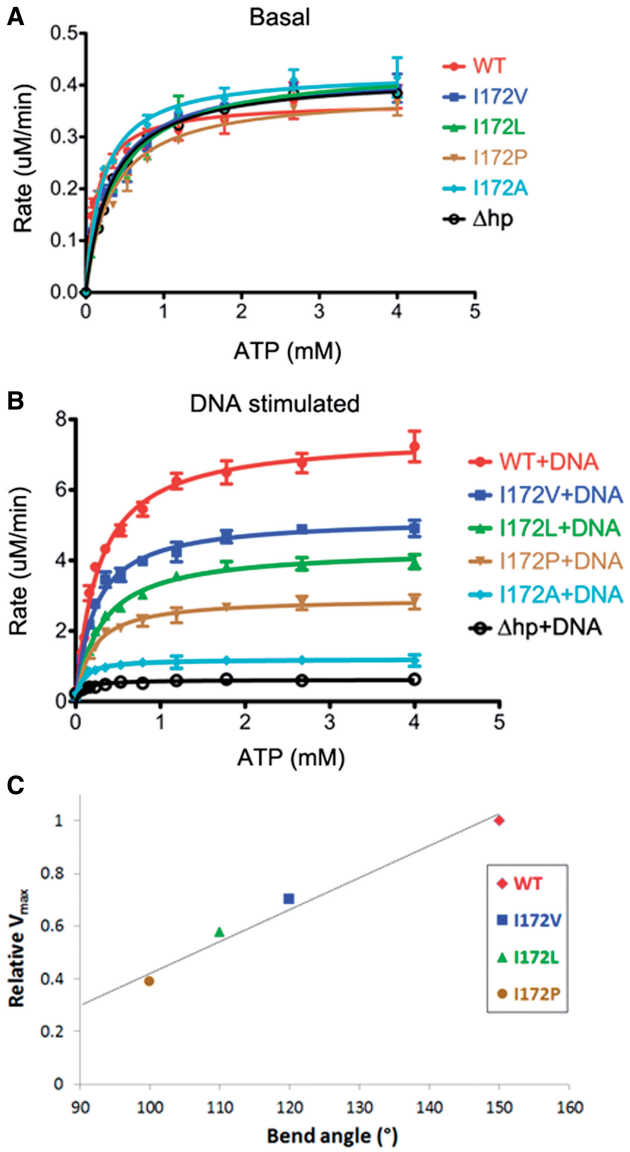

Figure 7. Ile_{172} is critical for supporting DNA-stimulated ATPase activity. The rates of ATP hydrolysis as catalyzed by wild-type topo IV, Ile_{172}Ala, Ile_{172}Pro, Ile_{172}Leu, Ile_{172}Val, and the Δhp construct are shown as a function of ATP concentration. ATPase rates were determined spectroscopically in the presence (**A**) or absence (**B**) of negatively supercoiled plasmid DNA. Data points represent the average of three independent experiments, with standard deviations shown as error bars. (**C**) Plot of observed V_{max} for ATP hydrolysis as a function of the calculated bend angles for the wild-type topo IV and selected topo IV variants. Data are not plotted for the Ile_{172}Ala, Ile_{172}Gly, Ile_{172}Trp or Δhp mutants, as bend angles could not be reliably derived from the low FRET signals seen for these constructs.

decatenation products beyond that seen in simple nicking/religation experiments (55). We initially set out to test this idea by mutating the conserved isoleucines to eliminate the ability of a model enzyme—in this instance, *E. coli* topo IV—to bend DNA. Instead, we discovered that even relatively conservative alterations to this amino acid markedly interfere both with positive and negative supercoil relaxation *in vitro* (Figures 2 and 3). Further biochemical investigations revealed that these changes did not generally affect DNA binding, but that they did severely disrupt DNA bending (Figures 5 and 6). Hence, the global DNA bend manifest by all type IIA topoisomerases studied to date is highly dependent on the dyad-related isoleucines that intercalate into the presumptive G-segment.

A precise DNA bend is integral to topo IV function

Although the demonstration of a causal link between the intercalative isoleucines and DNA bending was perhaps not so surprising (Figure 6), the impact of mutations at this site on the more global properties of topo IV was less expected. For example, alteration of Ile_{172} routinely diminished or abolished DNA supercoil relaxation (Figures 2 and 3) and DNA cleavage (Figure 4). Moreover, while Ile_{172} changes did not impact DNA affinity (Figure 5A), the loss of specific topo IV catalytic activities did correlate closely with the severity of the observed bending defects. Given the distance between the location of Ile_{172} and the respective sites of DNA cleavage, this finding indicates that the nucleolytic center of topo IV, and likely type IIA topoisomerases in general, is highly sensitive to the geometric configuration of DNA, and has evolved to work optimally with a precise degree of DNA deformation (Figure 8).

The deleterious effect of DNA-bending defects on the ATPase activity of topo IV also was unanticipated (Figure 7). The role of DNA in stimulating ATPase activity by type IIA topoisomerases has been well documented (33,51,57); however, this behavior generally has been attributed to G-segment binding, G-segment cleavage and/or T-segment binding. Our observation that a modest reduction in the global bend angle of DNA is capable of curbing DNA-stimulated ATP hydrolysis uncovers a new factor coupling efficient nucleotide turnover to normal enzyme function (Figure 8). This discovery adds to a growing number of coupling elements that have been identified to date in type IIA topoisomerases, such as the physical tether between the ATPase domain and the DNA binding and cleavage core in

Table 2. ATPase kinetic parameters for topo IV and mutants

Parameter	Topo IV					
	WT	Ile_{172}Val	Ile_{172}Leu	Ile_{172}Pro	Ile_{172}Ala	Δhp
DNA stimulated						
V_{max} (μM/min)	7.47 ± 0.16	5.21 ± 0.10	4.35 ± 0.08	2.93 ± 0.06	1.20 ± 0.04	0.62 ± 0.05
K_m (μM)	243 ± 27	221 ± 37	305 ± 29	252 ± 31	237 ± 19	211 ± 24
Basal						
V_{max} (μM/min)	0.39 ± 0.02	0.42 ± 0.02	0.44 ± 0.04	0.40 ± 0.03	0.43 ± 0.04	0.42 ± 0.05
K_m (μM)	353 ± 33	375 ± 41	391 ± 45	342 ± 28	298 ± 55	323 ± 51

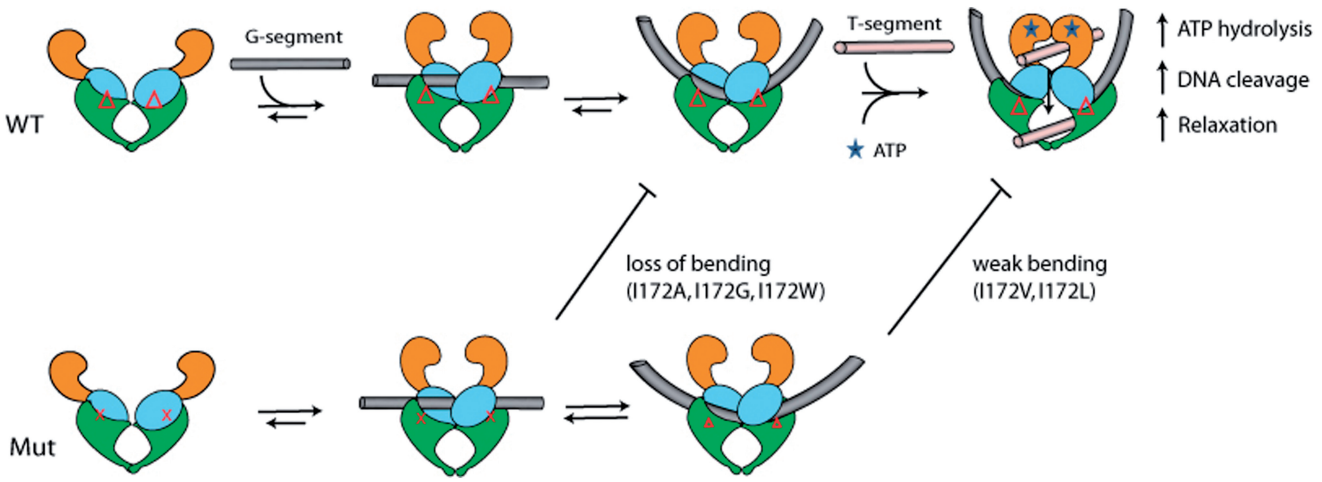

Figure 8. Schematic depicting the dependency of type IIA topoisomerase function on Ile_{172} and DNA bending. Different substitutions impair bending to different degrees; however, an inability to bend DNA to same extent as wild-type enzyme results in a defect in multiple topoisomerase activities. This scheme is in good agreement with a recently postulated 'DNA binding-bending-cleaving' model put forth by Lee *et al*. (56).

human topo IIα (58), the GyrA C-terminal domain tail (59), Mg^{2+}-ion–dependent DNA bending (56) and the K-loop in eukaryotic topo II (60). Taken together, these findings argue that type IIA topoisomerases are far more than a loosely tethered collection of disparate catalytic folds and activities, but rather a finely tuned system that uses a series of intramolecular sensors and actuators to ensure that DNA cleavage is tightly regulated and that ATP turnover is generally linked to productive strand passage events. Determining whether still additional control elements may exist, as well as understanding the physical and dynamic nature of the interplay between the linkage components identified thus far, constitute challenges for the future.

SUPPLEMENTARY DATA

Supplementary Data are available at NAR Online: Supplementary Table 1 and Supplementary Figures 1–5.

ACKNOWLEDGEMENTS

We would like to thank K. Drlica and the Berger laboratory for helpful discussions, and S. Vos for the expression vectors containing ParC and ParE.

FUNDING

National Cancer Institute [CA073773 to J.B.]. Funding for open access charge: National Cancer Institute.

Conflict of interest statement. None declared.

REFERENCES

1. Schoeffler,A.J. and Berger,J.M. (2008) DNA topoisomerases: harnessing and constraining energy to govern chromosome topology. *Q. Rev. Biophys.*, **41**, 41–101.
2. Forterre,P., Gribaldo,S., Gadelle,D. and Serre,M.C. (2007) Origin and evolution of DNA topoisomerases. *Biochimie*, **89**, 427–446.
3. Vos,S.M., Tretter,E.M., Schmidt,B.H. and Berger,J.M. (2011) All tangled up: how cells direct, manage and exploit topoisomerase function. *Nat. Rev. Mol. Cell. Biol.*, **12**, 827–841.
4. Wigley,D.B., Davies,G.J., Dodson,E.J., Maxwell,A. and Dodson,G. (1991) Crystal structure of an N-terminal fragment of the DNA gyrase B protein. *Nature*, **351**, 624–629.
5. Classen,S., Olland,S. and Berger,J.M. (2003) Structure of the topoisomerase II ATPase region and its mechanism of inhibition by the chemotherapeutic agent ICRF-187. *Proc. Natl Acad. Sci. USA*, **100**, 10629–10634.
6. Dutta,R. and Inouye,M. (2000) GHKL, an emergent ATPase/kinase superfamily. *Trends Biochem. Sci.*, **25**, 24–28.
7. Aravind,L., Leipe,D.D. and Koonin,E.V. (1998) Toprim—a conserved catalytic domain in type IA and II topoisomerases, DnaG-type primases, OLD family nucleases and RecR proteins. *Nucleic Acids Res.*, **26**, 4205–4213.
8. Berger,J.M., Gamblin,S.J., Harrison,S.C. and Wang,J.C. (1996) Structure and mechanism of DNA topoisomerase II. *Nature*, **379**, 225–232.
9. Morais Cabral,J.H., Jackson,A.P., Smith,C.V., Shikotra,N., Maxwell,A. and Liddington,R.C. (1997) Crystal structure of the breakage-reunion domain of DNA gyrase. *Nature*, **388**, 903–906.
10. Brown,P.O., Peebles,C.L. and Cozzarelli,N.R. (1979) A topoisomerase from *Escherichia coli* related to DNA gyrase. *Proc. Natl Acad. Sci. USA*, **76**, 6110–6114.
11. Gellert,M., Mizuuchi,K., O'Dea,M.H., Itoh,T. and Tomizawa,J.I. (1977) Nalidixic acid resistance: a second genetic character involved in DNA gyrase activity. *Proc. Natl Acad. Sci. USA*, **74**, 4772–4776.
12. Roca,J., Berger,J.M., Harrison,S.C. and Wang,J.C. (1996) DNA transport by a type II topoisomerase: direct evidence for a two-gate mechanism. *Proc. Natl Acad. Sci. USA*, **93**, 4057–4062.
13. Roca,J. and Wang,J.C. (1992) The capture of a DNA double helix by an ATP-dependent protein clamp: a key step in DNA transport by type II DNA topoisomerases. *Cell*, **71**, 833–840.
14. Roca,J. and Wang,J.C. (1994) DNA transport by a type II DNA topoisomerase: evidence in favor of a two-gate mechanism. *Cell*, **77**, 609–616.
15. Williams,N.L. and Maxwell,A. (1999) Probing the two-gate mechanism of DNA gyrase using cysteine cross-linking. *Biochemistry*, **38**, 13502–13511.
16. Harkins,T.T., Lewis,T.J. and Lindsley,J.E. (1998) Pre-steady-state analysis of ATP hydrolysis by Saccharomyces cerevisiae DNA

topoisomerase II. 2. Kinetic mechanism for the sequential hydrolysis of two ATP. *Biochemistry*, **37**, 7299–7312.
17. Kampranis,S.C., Bates,A.D. and Maxwell,A. (1999) A model for the mechanism of strand passage by DNA gyrase. *Proc. Natl Acad. Sci. USA*, **96**, 8414–8419.
18. Dong,K.C. and Berger,J.M. (2007) Structural basis for gate-DNA recognition and bending by type IIA topoisomerases. *Nature*, **450**, 1201–1205.
19. Rice,P.A., Yang,S., Mizuuchi,K. and Nash,H.A. (1996) Crystal structure of an IHF-DNA complex: a protein-induced DNA U-turn. *Cell*, **87**, 1295–1306.
20. Swinger,K.K., Lemberg,K.M., Zhang,Y. and Rice,P.A. (2003) Flexible DNA bending in HU-DNA cocrystal structures. *EMBO J.*, **22**, 3749–3760.
21. Wohlkonig,A., Chan,P.F., Fosberry,A.P., Homes,P., Huang,J., Kranz,M., Leydon,V.R., Miles,T.J., Pearson,N.D., Perera,R.L. *et al.* (2010) Structural basis of quinolone inhibition of type IIA topoisomerases and target-mediated resistance. *Nat. Struct. Mol. Biol.*, **17**, 1152–1153.
22. Bax,B.D., Chan,P.F., Eggleston,D.S., Fosberry,A., Gentry,D.R., Gorrec,F., Giordano,I., Hann,M.M., Hennessy,A., Hibbs,M. *et al.* (2010) Type IIA topoisomerase inhibition by a new class of antibacterial agents. *Nature*, **466**, 935–940.
23. Laponogov,I., Pan,X.S., Veselkov,D.A., McAuley,K.E., Fisher,L.M. and Sanderson,M.R. (2010) Structural basis of gate-DNA breakage and resealing by type II topoisomerases. *PLoS One*, **5**, e11338.
24. Schmidt,B.H., Burgin,A.B., Deweese,J.E., Osheroff,N. and Berger,J.M. (2010) A novel and unified two-metal mechanism for DNA cleavage by type II and IA topoisomerases. *Nature*, **465**, 641–644.
25. Vologodskii,A.V., Zhang,W., Rybenkov,V.V., Podtelezhnikov,A.A., Subramanian,D., Griffith,J.D. and Cozzarelli,N.R. (2001) Mechanism of topology simplification by type II DNA topoisomerases. *Proc. Natl Acad. Sci. USA*, **98**, 3045–3049.
26. Hardin,A.H., Sarkar,S.K., Seol,Y., Liou,G.F., Osheroff,N. and Neuman,K.C. (2011) Direct measurement of DNA bending by type IIA topoisomerases: implications for non-equilibrium topology simplification. *Nucleic Acids Res.*, **39**, 5729–5743.
27. Moore,C.L., Klevan,L., Wang,J.C. and Griffith,J.D. (1983) Gyrase . DNA complexes visualized as looped structures by electron microscopy. *J. Biol. Chem.*, **258**, 4612–4617.
28. Corbett,K.D., Schoeffler,A.J., Thomsen,N.D. and Berger,J.M. (2005) The structural basis for substrate specificity in DNA topoisomerase IV. *J. Mol. Biol.*, **351**, 545–561.
29. Osheroff,N. and Zechiedrich,E.L. (1987) Calcium-promoted DNA cleavage by eukaryotic topoisomerase II: trapping the covalent enzyme-DNA complex in an active form. *Biochemistry*, **26**, 4303–4309.
30. Rodriguez,A.C. (2002) Studies of a positive supercoiling machine. Nucleotide hydrolysis and a multifunctional 'latch' in the mechanism of reverse gyrase. *J. Biol. Chem.*, **277**, 29865–29873.
31. Bjornsti,M.A. and Megonigal,M.D. (1999) Resolution of DNA molecules by one-dimensional agarose-gel electrophoresis. *Methods Mol. Biol.*, **94**, 9–17.
32. Schneider,C.A., Rasband,W.S. and Eliceiri,K.W. (2012) NIH Image to ImageJ: 25 years of image analysis. *Nat. Methods*, **9**, 671–675.
33. Lindsley,J.E. and Wang,J.C. (1993) On the coupling between ATP usage and DNA transport by yeast DNA topoisomerase II. *J. Biol. Chem.*, **268**, 8096–8104.
34. Tamura,J.K. and Gellert,M. (1990) Characterization of the ATP binding site on *Escherichia coli* DNA gyrase. Affinity labeling of Lys-103 and Lys-110 of the B subunit by pyridoxal 5′-diphospho-5′-adenosine. *J. Biol. Chem.*, **265**, 21342–21349.
35. Mueller-Planitz,F. and Herschlag,D. (2007) DNA topoisomerase II selects DNA cleavage sites based on reactivity rather than binding affinity. *Nucleic Acids Res.*, **35**, 3764–3773.
36. Heyduk,T. and Lee,J.C. (1990) Application of fluorescence energy transfer and polarization to monitor *Escherichia coli* cAMP receptor protein and lac promoter interaction. *Proc. Natl Acad. Sci. USA*, **87**, 1744–1748.
37. Laponogov,I., Sohi,M.K., Veselkov,D.A., Pan,X.S., Sawhney,R., Thompson,A.W., McAuley,K.E., Fisher,L.M. and Sanderson,M.R. (2009) Structural insight into the quinolone-DNA cleavage complex of type IIA topoisomerases. *Nat. Struct. Mol. Biol.*, **16**, 667–669.
38. Wu,C.C., Li,T.K., Farh,L., Lin,L.Y., Lin,T.S., Yu,Y.J., Yen,T.J., Chiang,C.W. and Chan,N.L. (2011) Structural basis of type II topoisomerase inhibition by the anticancer drug etoposide. *Science*, **333**, 459–462.
39. Zechiedrich,E.L. and Cozzarelli,N.R. (1995) Roles of topoisomerase IV and DNA gyrase in DNA unlinking during replication in *Escherichia coli*. *Genes Dev.*, **9**, 2859–2869.
40. Peng,H. and Marians,K.J. (1993) Decatenation activity of topoisomerase IV during oriC and pBR322 DNA replication *in vitro*. *Proc. Natl Acad. Sci. USA*, **90**, 8571–8575.
41. Crisona,N.J., Strick,T.R., Bensimon,D., Croquette,V. and Cozzarelli,N.R. (2000) Preferential relaxation of positively supercoiled DNA by *E. coli* topoisomerase IV in single-molecule and ensemble measurements. *Genes Dev.*, **14**, 2881–2892.
42. Tse,Y.C., Kirkegaard,K. and Wang,J.C. (1980) Covalent bonds between protein and DNA. Formation of phosphotyrosine linkage between certain DNA topoisomerases and DNA. *J. Biol. Chem.*, **255**, 5560–5565.
43. Morrison,A. and Cozzarelli,N.R. (1979) Site-specific cleavage of DNA by *E. coli* DNA gyrase. *Cell*, **17**, 175–184.
44. Sugino,A., Higgins,N.P. and Cozzarelli,N.R. (1980) DNA gyrase subunit stoichiometry and the covalent attachment of subunit A to DNA during DNA cleavage. *Nucleic Acids Res.*, **8**, 3865–3874.
45. Peng,H. and Marians,K.J. (1995) The interaction of *Escherichia coli* topoisomerase IV with DNA. *J. Biol. Chem.*, **270**, 25286–25290.
46. Ha,T., Rasnik,I., Cheng,W., Babcock,H.P., Gauss,G.H., Lohman,T.M. and Chu,S. (2002) Initiation and re-initiation of DNA unwinding by the *Escherichia coli* Rep helicase. *Nature*, **419**, 638–641.
47. Mizuuchi,K., Fisher,L.M., O'Dea,M.H. and Gellert,M. (1980) DNA gyrase action involves the introduction of transient double-strand breaks into DNA. *Proc. Natl Acad. Sci. USA*, **77**, 1847–1851.
48. Liu,L.F., Liu,C.C. and Alberts,B.M. (1980) Type II DNA topoisomerases: enzymes that can unknot a topologically knotted DNA molecule via a reversible double-strand break. *Cell*, **19**, 697–707.
49. Goto,T. and Wang,J.C. (1982) Yeast DNA topoisomerase II. An ATP-dependent type II topoisomerase that catalyzes the catenation, decatenation, unknotting, and relaxation of double-stranded DNA rings. *J. Biol. Chem.*, **257**, 5866–5872.
50. Cozzarelli,N.R. (1980) DNA gyrase and the supercoiling of DNA. *Science*, **207**, 953–960.
51. Mizuuchi,K., O'Dea,M.H. and Gellert,M. (1978) DNA gyrase: subunit structure and ATPase activity of the purified enzyme. *Proc. Natl Acad. Sci. USA*, **75**, 5960–5963.
52. Osheroff,N. (1986) Eukaryotic topoisomerase II. Characterization of enzyme turnover. *J. Biol. Chem.*, **261**, 9944–9950.
53. Anderson,V.E., Gootz,T.D. and Osheroff,N. (1998) Topoisomerase IV catalysis and the mechanism of quinolone action. *J. Biol. Chem.*, **273**, 17879–17885.
54. Buck,G.R. and Zechiedrich,E.L. (2004) DNA disentangling by type-2 topoisomerases. *J. Mol. Biol.*, **340**, 933–939.
55. Rybenkov,V.V., Ullsperger,C., Vologodskii,A.V. and Cozzarelli,N.R. (1997) Simplification of DNA topology below equilibrium values by type II topoisomerases. *Science*, **277**, 690–693.
56. Lee,S., Jung,S.R., Heo,K., Byl,J.A., Deweese,J.E., Osheroff,N. and Hohng,S. (2012) DNA cleavage and opening reactions of human topoisomerase IIalpha are regulated via Mg2+-mediated dynamic bending of gate-DNA. *Proc. Natl Acad. Sci. USA*, **109**, 2925–2930.
57. Osheroff,N., Shelton,E.R. and Brutlag,D.L. (1983) DNA topoisomerase II from Drosophila melanogaster. Relaxation of supercoiled DNA. *J. Biol. Chem.*, **258**, 9536–9543.

58. Bjergbaek,L., Kingma,P., Nielsen,I.S., Wang,Y., Westergaard,O., Osheroff,N. and Andersen,A.H. (2000) Communication between the ATPase and cleavage/religation domains of human topoisomerase IIalpha. *J. Biol. Chem.*, **275**, 13041–13048.
59. Tretter,E.M. and Berger,J.M. (2012) Mechanisms for defining the supercoiling setpoint of DNA gyrase orthologs I. A non-conserved acidic C-terminal tail modulates *E. coli* gyrase activity. *J. Biol. Chem.*, **287**, 18636–18644.
60. Schmidt,B.H., Osheroff,N. and Berger,J.M. (2012) Structure of a topoisomerase II-DNA-nucleotide complex reveals a new control mechanism for ATPase activity. *Nat. Struct. Mol. Biol.*, **19**, 1147–1154.